



**HAL**  
open science

# A Study of Fish Undulatory Swimming Based on Merged CFD and Experimental Video of the Swimming Movement of Mosquito Fish

Jiashun Guan, Penanklihi Kone, Gurvan Jodin, Xiangyi Tang, Dixia Fan, Sparsh Agarwal, Haishuo Chen, Jiarui Yang, James Herbert-Read

► **To cite this version:**

Jiashun Guan, Penanklihi Kone, Gurvan Jodin, Xiangyi Tang, Dixia Fan, et al.. A Study of Fish Undulatory Swimming Based on Merged CFD and Experimental Video of the Swimming Movement of Mosquito Fish. OCEANS 2021, Sep 2021, San Diego, United States. pp.1-6, 10.23919/OCEANS44145.2021.9705744 . hal-04289932

**HAL Id: hal-04289932**

**<https://hal.science/hal-04289932>**

Submitted on 19 Nov 2023

**HAL** is a multi-disciplinary open access archive for the deposit and dissemination of scientific research documents, whether they are published or not. The documents may come from teaching and research institutions in France or abroad, or from public or private research centers.

L'archive ouverte pluridisciplinaire **HAL**, est destinée au dépôt et à la diffusion de documents scientifiques de niveau recherche, publiés ou non, émanant des établissements d'enseignement et de recherche français ou étrangers, des laboratoires publics ou privés.

# A Study of Fish Undulatory Swimming Based on Merged CFD and Experimental Video of the Swimming Movement of Mosquito Fish

Jiashun Guan  
*Department of Mechanics and Engineering  
Science  
Peking University  
Beijing, China  
jiashun@stu.pku.edu.cn*

Penanklihi Kone  
*ENS Rennes  
Rennes, France  
penanklihi.kone@ens-rennes.fr*

Gurvan Jodin\*  
*SATIE CNRS  
ENS Rennes  
Rennes, France  
gurvan.jodin@ens-rennes.fr*

Xiangyi Tang  
*Shanghai Pinghe School  
Shanghai, China  
tanxgaingyi13@163.com*

Dixia Fan  
*Queens University  
ON, Canada  
dixia.fan@QUEENSU.CA*

Sparsh Agarwal  
*Birla Institute of Technology and Science  
Pilani, India  
sparshagarwal018@gmail.com*

Haishuo Chen  
*Renmin University of China  
Beijing, China  
chenhaishuo1999@163.com*

Jiarui Yang  
*Shanghai Pinghe School  
Shanghai, China  
jiarui.andrew.yang@outlook.com*

James Herbert-Read  
*University of Cambridge  
Cambridge, England  
jh2223@cam.ac.uk*

**Abstract**—significant progress has been made to improve the agility of the aquatic vehicles via bio-inspired design and control. Compared to propeller and rudder used in traditional rigid vehicles, fish undulatory motion shows great properties in utilizing surrounding hydrodynamical conditions to achieve a more efficient locomotion. Many parametric models have been established to explore propulsive mechanism of fish swimming in previous literatures. However, fish undulatory motion observed in experiments indicates it is much more complex than parametric models. We developed a new image processing tools to capture fish kinematics characters from the live fish experiments video. A data interpretation method has also been implemented to transfer real fish geometry and kinematics to 2D CFD simulation platform from experiment data, which gives a reliable way to visualize wake vortices pattern and analyze hydrodynamical interaction. Wake vortices in steady swimming phase and lateral vortices in zigzag swimming phase can be observed clearly through a demo fish swimming experiments video and above methods. These vortices have a strong self induced velocity to travel side way and evolve for a long duration.

**Keywords**—swimming fish, flow visualization, underwater machine, vortex stress, hydrodynamics

## I. INTRODUCTION

Since the 1990s, due to the improvement of mechanical engineering, many researchers started to take closer studies on the swimming movements of fish<sup>[1]</sup>. These studies have important significance for the creation and implementation of more efficient underwater machines and robots. In the environmental engineering field, these studies help people

identify the habitat needs and migration patterns of different types of fish<sup>[2], [3]</sup>.

In the past, physics studies mainly focused on the vortex street formation and the near-wake flow around bluff bodies<sup>[4], [5], [6]</sup>. Scientists have realized the efficiency of fish swimming is very high and fishes are able to swim at a speed which exceeds the maximum velocity provided by muscle power. It turns out that fish are able to exploit energy from near-by vortices<sup>[7]</sup>. Meanwhile, scientists are also interested in the hydrodynamics of fish-like swimming. Principles of fish-like swimming such as vorticity control have been investigated<sup>[8], [9]</sup>. In addition, fish swimming has been classified into different modes such as thunniform, anguilliform, subcarangiform, and carangiform. This classification makes the study of fish motion more organized<sup>[10], [11]</sup>. So far, a lot of research focuses on the parameters such as wavelength of fish motions under different Strouhal numbers<sup>[12], [13], [14]</sup>. Additionally, extraordinary theoretical equations are gained<sup>[15], [16]</sup>.

The experiment design has conspicuous inaccuracies in most of the previous studies. First, the previous sensors could not captivate or record the accurate movements of the fish. As fish are moving creatures in a 3-dimensional world, it was difficult for previous equipment to observe and record the data. Therefore, it would be impossible for the researchers to capture the intricacies of the fish locomotion. Moreover, as living fish are uncontrollable, researchers had to use fake fish to simulate their movements, which would be different from how fish swim and move in the real world, leading to large inaccuracies in the research statistics. The conclusions

remained theoretical and limited, with a large deviation from the real world situations. Besides, fluid mechanics is one of the most complicated, which increases the difficulty to analyze the fish locomotion. The oscillation of the fish's tail movement created whirlpools, where the same fish could draw energy. The mutual influence further complicates the model.

In order to get more practical research results, our team has designed and conducted research using living fish as models and analyzed them using motion graphics. As the code could retain the swimming model of the real fish, our team used Lily Pad simulation platform<sup>[17]</sup> to simulate fish hydrodynamics flow. The rest of the paper is organized as follows, we first present in the section Materials and Methods the motion capture algorithm as well as the numerical simulation environment. Then we demonstrate in Result and Discussion the wake pattern around and behind a single fish in two phases: steady swimming phase, zig-zag phase, as well as the long-term far vortical wake left by the moving fish.

## II. METHODS AND MATERIALS

### A. MODELING FISH MOTION FROM EXPERIMENTAL VIDEOS

To overcome the problem of unrealistic modeling of fish motion, we adopt a code to extract fish motion from video. The code works in three steps: load a video and extract sub-images of fishes; fit fish model for each sub-images; merge all the data into a unique file. As a benchmark, a 2 second video which contains a top view of the motion of 2 mosquitofish (*Gambusia affinis*) evolving in shallow water is chosen. Fig. 1 presents one frame of this video. The analysis of this video not only helps us simulate the motion of a single fish, but also gives us insight into the swimming pattern of a group of fishes.

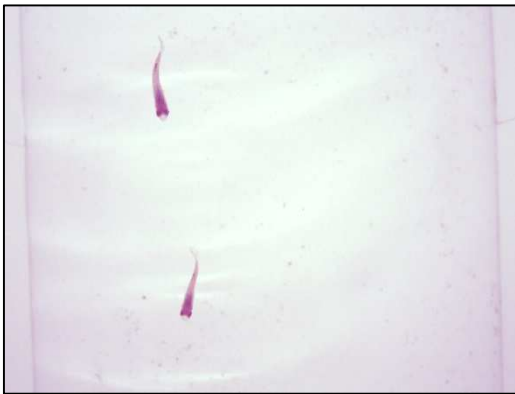


Fig. 1 one frame of the benchmark video. The two mosquito fishes are swimming in shallow water

The first step is to extract the fish images from the video. To do this, for each frame of the video, a K-means algorithm is used to process the image to isolate the fishes from the moving background. Then, additional filtering processing is used to precisely locate the fish in the image. The K-means algorithm is a clustering algorithm. It allows segmenting data into K distinct clusters. In the case of an image, similar pixels are found in a cluster, in an exclusive way. The algorithm, although old<sup>[18]</sup>, its modern versions are very frequently

used<sup>[19],[20]</sup>. To segment the image into K distinct clusters, the K-means algorithm needs a criterion to express the degree of similarity between the different pixels. The Manhattan distance is used to determine the similarity of 2 pixels; and the number of clusters is fixed at 2 to avoid a too fragmented partitioning of the image. The K-means fitting allows to clean the image, so a simple binarization by threshold produces satisfactory results to keep only the silhouettes of the fish. The result is a binary image on which a Canny filter will be applied. The Canny filter is used to detect contours<sup>[21]</sup>. These contours will define a rectangle delimiting the fish in the image. The contents of these rectangles define subimages containing one fish that will be used as a basis for the interpolation algorithms of the next step.

After identifying subimages with fishes in each frame, a deformed NACA profile is used to model the fish, thanks to optimization. The objective of interpolation by optimization is to start from an ideal profile and to optimize its parameters to approximate the real fish. For this optimization, we choose a NACA 0008 type profile of fixed chord. The parameters chosen for the optimization are: the rotation  $\theta$ , translation  $(tx, ty)$  and deformation of the mean line with control points  $y_i$ . The mean line of the deformed profile is shaped as a spline parametrized by the control points. These control points have  $N$  equally spaced abscisses along the profile chord, with corresponding  $N$  ordinates  $y_i$ . The interpolated spline defines a continuous ordinate deviation that is applied to the NACA profile. Fig. 2 illustrates the rotation, translation and deformation of the profile at the different steps of the optimization algorithm described in the following.

Now the fishes deformations and motions are modeled, a regression is performed on each subimages of fishes extracted from the video. To do so, an optimization algorithm is implemented. A criteria - i.e. cost function to be optimized - is defined. In other words, a cost function  $J$  will be here is of the form  $J(\theta, tx, ty, p_i, Y)$  where  $Y$  denotes the matrix image of the real fish; the parameters  $tx, ty, \theta, p_i$  are those defined before. Two cost functions are considered: common area, and area difference. The ‘‘Common area’’ cost function is the intersection between the NACA profile area and the real fish area, to be maximized. Binary images are used. The ‘‘Area difference’’ aims at minimizing the area difference between the surface of the real fish and the surface of the NACA profile. A Gaussian blur is used on the images to get a progressive objective function, enhancing algorithm convergence.

The optimization problem consists of optimizing the parameters  $\theta, tx, ty,$  and  $p_i$  with constraints to approximate the shape of the actual fish. This problem can be formulated as follows:

$$\begin{aligned} & \text{minimize } J(\theta, tx, ty, p_i, Y) \\ & \theta, tx, ty, p_i \\ & \text{subject to: } \quad -0.2 \leq \theta \leq 2\pi \\ & \quad \quad \quad -1 \leq tx, ty \leq 1 \\ & \quad \quad \quad |p_i| \leq 0.5 \end{aligned}$$

The optimization is done sequentially. Fig. 2 presents the results for the two steps. The first step is to optimize the rotation ( $\theta$ ) translation ( $t_x$ ,  $t_y$ ) parameters. Then the optimization of the polynomial deformation. If the looping condition is satisfied (e.g. a condition on the overall cost) then another optimization cycle is started in succession. Powell's method is used, as it is a global optimization algorithm under constraints which allows to minimize a function of several variables. Here the function to be minimized is the cost function  $J$ . This algorithm is studied in more detail in [22].

Once the subimages of individual fishes are extracted from the video, and they are modeled by deformed NACAs, the last step is to combine all the results in one file per fish. These files contain the global location of the fish model, plus rotation and deformation splines, for each frame. These files can therefore be imported to the fluid dynamic simulation platform.

Finally, optimization results are saved in a "xxx\_MODEL.csv" file. Before the saving, datas are checked for their consistency to ensure the reliability of parameters. Using those parameters, a NACA spinal simulation can be drawn in a coordinate- plane and the motion of fish can be determined.

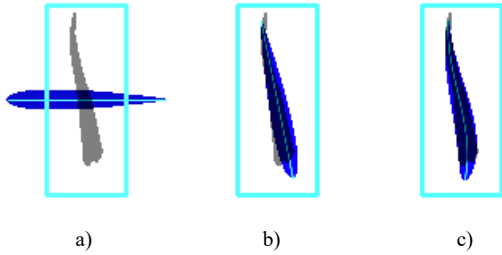


Fig. 2 Optimization steps. a) initial state. b) optimal rotation and translation. c) optimal deformation with previous optimal rotation and translation. The blue profile is the model, the clear blue outbox contains the binary picture of the fish in grey.

## B. COMPUTATIONAL FLUID DYNAMICS PLATFORM: LILY PAD CFD

Fish body has extremely significant flexibility, which makes body-fluid interaction complex and various in different parts of body. Lily Pad is a robust method for dealing with fluid-solid coupling cases by using Boundary Data Immersion Method (BDIM) [21]. It convolves two governing equations of fluid and body domain by a delta kernel  $K_\epsilon$  with width  $\epsilon$ :

$$\vec{u}_\epsilon(\vec{x}) = \mu_0^\epsilon \vec{f} + (1 - \mu_0^\epsilon) \vec{b} + \mu_1^\epsilon \frac{\partial}{\partial n} (\vec{f} - \vec{b}) \quad (1)$$

where  $\vec{f}$  and  $\vec{b}$  are the update equations for the velocity in the fluid and body domains, and where  $\mu_0$  and  $\mu_1$  are the zeroth and first moments of the kernel function with respect to the fluid domain [17]. The 2nd order BDIM formulation shows a versatile and accurate property for intermediate Reynolds number applications like biomimetic locomotion. Moreover, Lily Pad decreases the barrier to CFD and can be friendlier for researchers with little CFD skills.

We set up mesh number in width and height as  $2^8=256$ , fish length as 38 meshes and time step  $dt$  as 0.0149s which is interval of two video frames. For pre-treatment, we wrote a MATLAB program to convert the fish vertebral line given by the code mentioned above from relative coordinate to global coordinate. A top view of four body outlines and fish head trajectory are drawn in global coordinate as Fig. 3, which shows great consistence with the benchmark video. We created a new class of Lily Pad named 'Livefish'. This class gives body outline in every time steps by using global coordinate of control points locations. Class 'Livefish' also utilizes an interpolation method, shown as Fig. 4, to extract body velocity as an input of BDIM, which is one of the most important custom parts for Lily Pad solver. For a random point located at one segment of body outline between two control points, we defined a parameter  $\alpha_i$ ,  $i=1,2$  to indicate the ratio of  $AP_i$  and  $AB_i$ , where  $AP_i$  is distance projection of this point to one endpoint of such segment,  $AB_i$  is length projection of such segment and index  $i$  represents the projection in two dimension. We can easily get the location of this point in the last time step by keeping  $\alpha_i$  consistent. Body velocity is obtained by a vector from the last time step location to this time step location and  $dt$ .

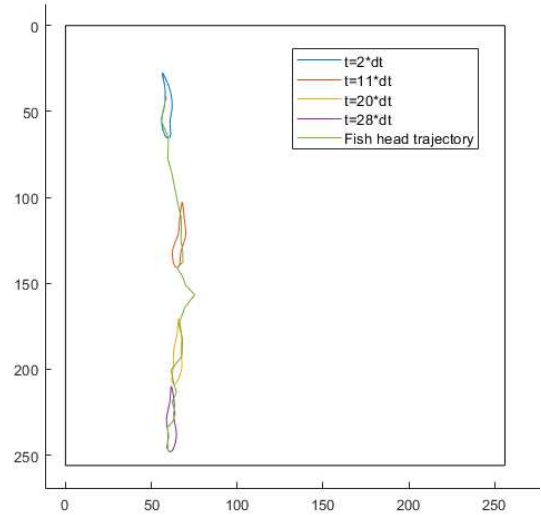


Fig.3 Fish body outlines and fish head trajectory

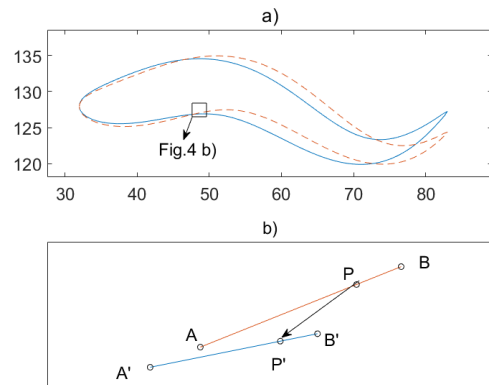


Fig.4 a sketch of the interpolation method. a) a global view. b) a local view. Vector  $PP'$  is the displacement vector.

### III. RESULTS AND DISCUSSION

In this section, we present the result of the simulated flow pattern of a single fish, which helps to shed some light on the motion in the live fish experiment.

Four Y-direction velocity profiles are shown in Fig. 5 b). These profiles are located at black line in Fig. 5 a), a third of fish length behind fish tail. Unlike parametric models of fish locomotion in previous literatures [26], [27], [28], driving force of live fish is fluctuating. They undulate the body for gaining locomotion and slide with a minimum drag force body shape. When driving force is larger than drag force, the Y-direction velocity profile behind fish tail looks like a jet as Fig.5 b) (4) shows. Instead, the profile is shown as Fig.5 b) (2), like a reverse-jet. We selected static velocity field as initial field. That's why Fig.5 b) (1) shows a centrosymmetric velocity profile of a single vortex. A Y-velocity profile of fish turning state is also shown in Fig.5 b) (3). Zigzag fish swimming will be detailed in the following.

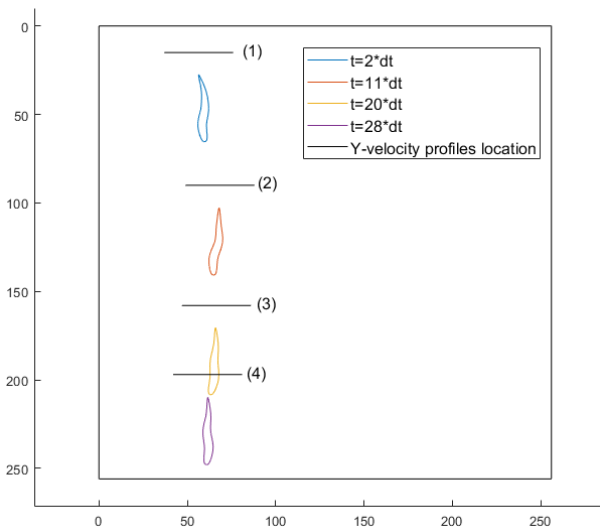


Fig5. a) Y-velocity profiles location

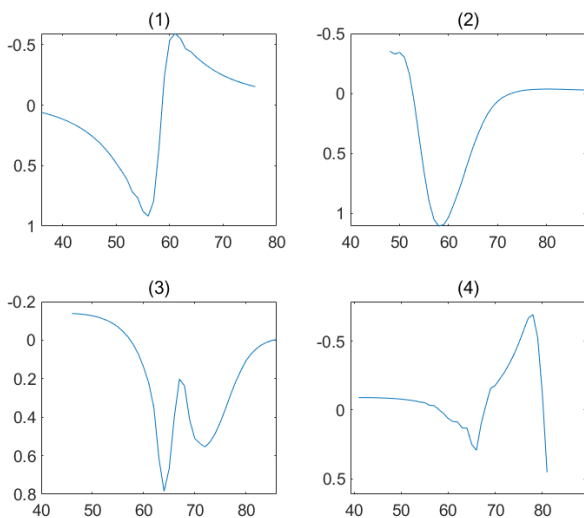


Fig.5 b) four Y-direction velocity profiles

#### A. STEADY SWIMMING PHASE

The following four figures from Fig.6-Fig.9 are vorticity field versus the benchmark video frame at four moments in uniform swimming state.

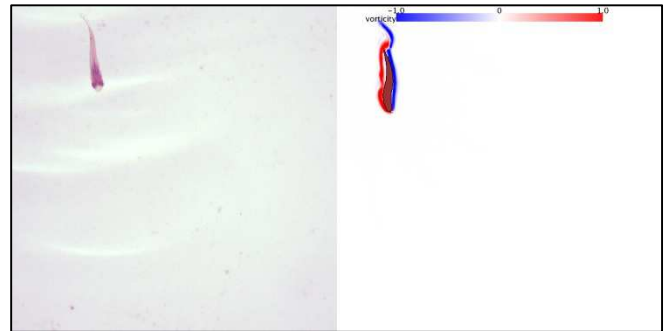


Fig. 6  $t=0.0298s$ . a) the benchmark video.  
b) vorticity simulation by Lily Pad.

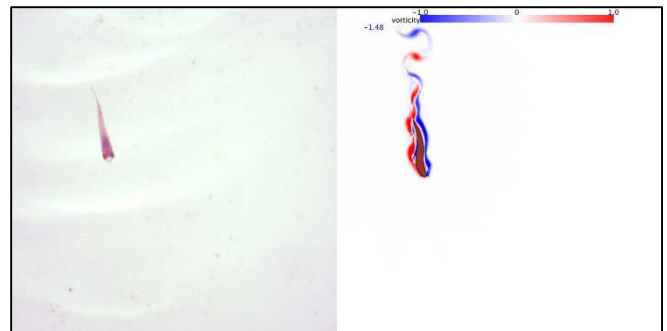


Fig. 7  $t=0.0894s$ . a) the benchmark video.  
b) vorticity simulation by Lily Pad.

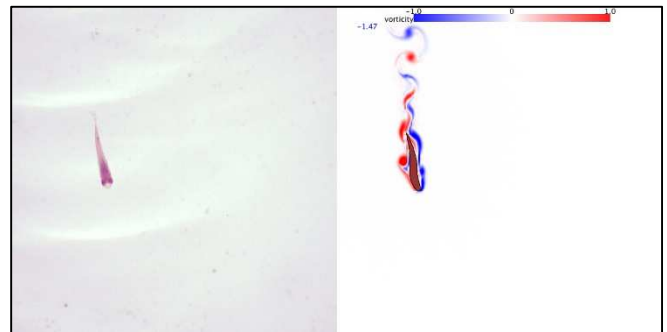


Fig. 8  $t=0.1043s$ . a) the benchmark video.  
b) vorticity simulation by Lily Pad.

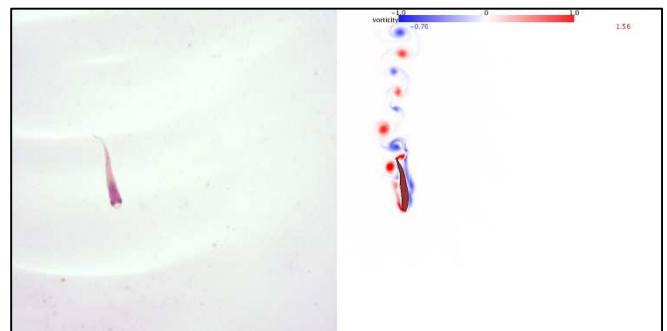


Fig. 9  $t=0.1788s$ . a) the benchmark video.  
b) vorticity simulation by Lily Pad.

### B. STEADY SWIMMING PHASE

By creating a lateral vortex, fish can realize zigzag swimming and turning around. We can observe a lateral vortex forming and clinging to the fish tail in Fig.10. At the upper left, an already formed lateral vortex in a red circle is moving forward.

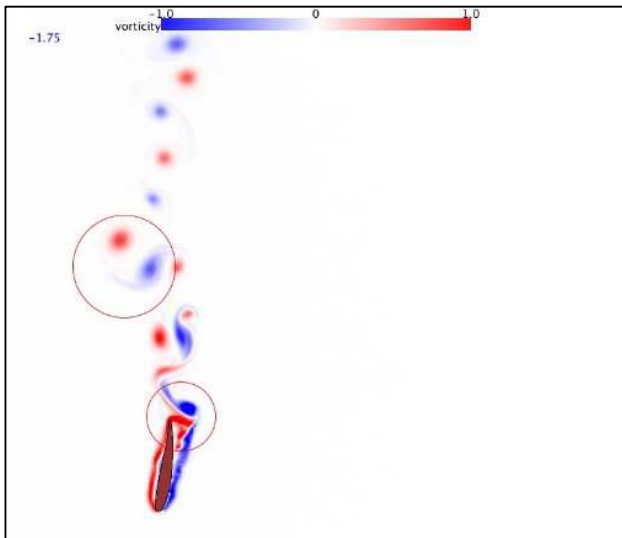


Fig.10 lateral vortex forming in zigzag swimming.

### C. FISH DOWNSTREAM WAKE EVOLUTION

After the fish has left the experimental area / numerical zone, we let the simulation run for another 0.298s. It is found that the vortical wake left behind in the single fish is well captured for a long time duration by the current simulation tool. The result is shown in Fig. 11 and it can be seen that the vortex pair generated by the fish in the zigzag phase has a strong self induced velocity and therefore travels side way, while the vortex street left by the fish in the steady swimming phase is relatively steady.

The result demonstrates the capability of the code of well preserving the vortical wake behind the fish, providing the future potential to study the multiple fish interaction.

### IV. CONCLUSION

In this work, we demonstrate the capability of combining live fish experiments, camera motion identification algorithm and computational fluid simulation tools to study the hydrodynamics of the real fish movement in the fluid. Through a demo of a single fish swimming experiment, it is clear to see that the vortical wake pattern can be easily provided by the simulation but is difficult to acquire in the live fish experiments, which can help the biologist to shed great light on the fish behavior. Though the current work presents only the preliminary result, and requires more attention for detailed fluid mechanics validation and analysis, it paves a great potential for future fish biological motion research.

### V. ACKNOWLEDGEMENT

We wish to acknowledge the funding support of the research initiation grant provided by Queen's University and NERSC Discovery Grant. We wish to acknowledge the computational resource provided by Compute Canada.

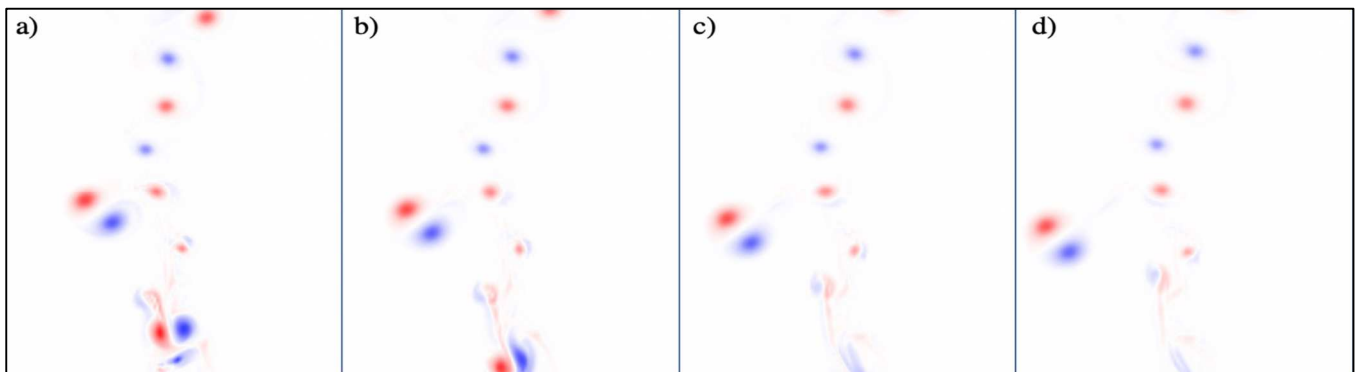


Fig.11 vortical wake ( $t=0.44849s$ ,  $t=0.52299s$ ,  $t=0.59749s$ ,  $t=0.67199s$ ).

## REFERENCES

- [1] J. Q. Maggs, and P. D. Cowley. "Nine decades of fish movement research in southern Africa: a synthesis of research and findings from 1928 to 2014." *Reviews in Fish Biology and Fisheries* 26.3 (2016): 287-302.
- [2] Cathcart, C. N., Gido, K. B., McKinstry, M. C., and MacKinnon, P. D. "Patterns of fish movement at a desert river confluence. *Ecology of Freshwater Fish*", 27(1), (2018): 492-505.
- [3] Carpenter-Bundhoo, L., et al. "Reservoir to river: Quantifying fine-scale fish movements after translocation." *Ecology of Freshwater Fish* 29.1 (2020): 89-102.
- [4] Roshko, A. "On the wake and drag of bluff bodies." *Journal of the aeronautical sciences* 22.2 (1955): 124-132.
- [5] Wang, J., Fan D., and Lin K.. "A review on flow-induced vibration of offshore circular cylinders." *Journal of Hydrodynamics* 32.3 (2020): 415-440.
- [6] Fan, D., Wang, Z., Triantafyllou, M. S. and Karniadakis, G. E. "Mapping the properties of the vortex-induced vibrations of flexible cylinders in uniform oncoming flow". *Journal of Fluid Mechanics*, 881, (2019): 815-858.
- [7] Liao, J. C., Beal, D. N., Lauder, G. V., and Triantafyllou, M. S. "Fish exploiting vortices decrease muscle activity". *Science*, 302(5650), (2003): 1566-1569.
- [8] Triantafyllou, M. S., Triantafyllou G. S., and D. K. P. Yue. "Hydrodynamics of fishlike swimming." *Annual review of fluid mechanics* 32.1 (2000): 33-53.
- [9] Fish, F/, and Lauder G. "Passive and active flow control by swimming fishes and mammals." *Annu. Rev. Fluid Mech.* 38 (2006): 193-224.
- [10] Sfakiotakis, M., David M. L., and Davies J. B. C.. "Review of fish swimming modes for aquatic locomotion." *IEEE Journal of oceanic engineering* 24.2 (1999): 237-252.
- [11] Rosenberger, L. J. "Pectoral fin locomotion in batoid fishes: undulation versus oscillation." *Journal of Experimental Biology* 204.2 (2001): 379-394.
- [12] Nangia, N., Bale, R., Chen, N., Hanna, Y., and Patankar, N. A. "Optimal specific wavelength for maximum thrust production in undulatory propulsion". *PloS one*, 12(6), (2017): e0179727.
- [13] Eloy, C. "Optimal Strouhal number for swimming animals." *Journal of Fluids and Structures* 30 (2012): 205-218.
- [14] Taylor, G. K., Robert L. N., and Thomas, A. L. "Flying and swimming animals cruise at a Strouhal number tuned for high power efficiency." *Nature* 425.6959 (2003): 707-711.
- [15] Lighthill, M. J. "Note on the swimming of slender fish." *Journal of fluid Mechanics* 9.2 (1960): 305-317.
- [16] Lighthill, M. J. "Hydromechanics of aquatic animal propulsion." *Annual review of fluid mechanics* 1.1 (1969): 413-446.
- [17] Weymouth, G. D. "Lily pad: Towards real-time interactive computational fluid dynamics." *arXiv preprint arXiv:1510.06886* (2015).
- [18] Hartigan, J. A., and Manchek A. W. "Algorithm AS 136: A k-means clustering algorithm." *Journal of the royal statistical society. series c (applied statistics)* 28.1 (1979): 100-108.
- [19] Fan, D., Wu, B., Bachina, D., and Triantafyllou, M. S. "Vortex-induced vibration of a piggyback pipeline half buried in the seabed". *Journal of Sound and Vibration*, 449, (2019): 182-195.
- [20] Fan, D., and Triantafyllou, M. S. "Vortex induced vibration of riser with low span to diameter ratio buoyancy modules." In *The 27th International Ocean and Polar Engineering Conference*. OnePetro. (2017).
- [21] Canny, J. "A computational approach to edge detection." *IEEE Transactions on pattern analysis and machine intelligence* 6 (1986): 679-698.
- [22] Floudas, C. A., and Pardalos P. M., eds. *Encyclopedia of optimization*. Springer Science & Business Media, 2008.
- [23] Maertens, A. P., and Weymouth, G. D. "Accurate Cartesian-grid simulations of near-body flows at intermediate Reynolds numbers." *Computer Methods in Applied Mechanics and Engineering* 283 (2015): 106-129.
- [24] Fan, D., Zhang, X., and Triantafyllou, M. S. "Drag coefficient enhancement of dual cylinders in oscillatory flow". In *The 27th International Ocean and Polar Engineering Conference*. OnePetro. (2017).
- [25] Wang, J., and Fan, D. "An active learning strategy to study the flow control of a stationary cylinder with two asymmetrically attached rotating cylinders". In *The 30th International Ocean and Polar Engineering Conference*. OnePetro. (2020).
- [26] Videler, J. J., and Hess, F. "Fast continuous swimming of two pelagic predators, saithe (*Pollachius virens*) and mackerel (*Scomber scombrus*): a kinematic analysis." *Journal of experimental biology* 109.1 (1984): 209-228.
- [27] Tytell, E. D., and Lauder, G V. "The hydrodynamics of eel swimming: I. Wake structure." *Journal of Experimental Biology* 207.11 (2004): 1825-1841.
- [28] Ebrahimi, M., and Abbaspoor, M. "Imitation of the body/caudal fin undulatory swimming of a spiny dogfish (*Squalus acanthias*): The kinematic equation." *Proceedings of the Institution of Mechanical Engineers, Part M: Journal of Engineering for the Maritime Environment* 230.2 (2016): 388-403.